- Point of injection - WWall and Center:
  There are differences s in D_L obtained for a given process rate, from a wall injection and a center i injection response. For example, considering the injection at nozzle N1; N1 - wwall yields higher dispersion coefficients than N1 - center. This occurs because t the tracer injected at the wall is carried down sooner by the downflowing liquiiid at the wall, while for the center injection of the tracer, the liquid tracer is trransported down predominantly by the turbulent motion, and its arrival by connvection is retarded as it first has to reach the top of the reactor. When the trracer arrives earlier, the apparent dispersion coefficient is larger. Similarly for tthe injection at nozzle N2, which is at the bottom of the reactor, D_L obtained frrom the center injection response is higher since the tracer is carried up to the ddetector faster by upward convection of the liquid in the core region of the colulumn.

The effects discussed are mmost prominent for the lowest superficial gas velocity, i.e., run 14.7, and are found to ddecrease with increasing gas velocity. This is to be expected as turbulent mixing starts t to dominate convective effects at high gas velocity.

In order to quantitativelely assess the differences in the various D_L values obtained for a given process rate, a a statistical analysis is carried out using the ANalysis Of VAriances (ANOVA). Detaiails of the analysis are presented in Appendix IV. The D_L values from a particular innjection response are considered to belong to a group or treatment. The differences i in the D_L's from within the treatment (the values obtained at different detector levels)s) are considered to arise due to random error within the treatment. For each run t there are four such treatments due to the measurements from four injection points (t(top - center and wall, and bottom - center and wall). The purpose of the analysis is tto determine if there are any significant differences in the averages of the different trreatments. This is done by comparing the variances in the treatment means with the vvariance within each treatment. The results of this analysis (Appendix IV, Table A.4.11) suggest that for runs 14.6 and 14.7 the four treatment means (three for run 14.6)) are significantly different so that they belong to different classes, whereas for run 14.1.8 they all belong to the same category. The results from ANOVA thus confirm our r earlier assertion that the differences in the D_L obtained from the top and bottom iinjection and the center and side injections are real. This means that the liquid flow a and mixing phenomena cannot be captured adequately by the axial dispersion model l (ADM), except perhaps at the highest gas velocity. The results for the mean $\overline{D_L}$ forr all treatments in each run are reported in Table 3, along

Table 2: Parameeters for Liquid Phase Tracer Experiments

Run No.	U_G cm/s	P MPa	Gas Holdup	Injection	Det. Lev.	D_L cm^2/s
14.6	25.3	5.2	0.39	N1 - CEN	1	2879
					2	2751
					3	2717
				N1 - WAL	1	3563
					2	5433
					3	5776
				N2 - CEN	5	7081
					6	4313
					7	4696
				N2 - WAL	5	not
					6	avai-
					7	lable
14.7	14.1.3	5.2	0.33	N1 - CEN	1	1828
					2	2045
					3	1962
				N1 - WAL	1	2466
					2	3183
					3	3377
				N2 - CEN	5	4171
					6	2831
					7	3051
				N2 - WAL	5	2911
					6	2465
					7	2270
14.8	36.3.0	3.6	0.37	N1 - CEN	1	4432
					2	5117
					3	4742
				N1 - WAL	1	4924
					2	5331
					3	5403
				N2 - CEN	5	5501
					6	5163
					7	5925
				N2 - WAL	5	4741
					6	4441
					7	5991

with the standard deviatioons $\overline{\sigma_L}$ [1].

In order to study the effffect of superficial gas velocity on the dispersion coefficient, and assess whether any statistically significant variation exists, given that the values vary so widely in a given rurun, a similar analysis (ANOVA) is performed. In this case, the D_L from all injection responses of a given run were considered to belong to a single group or treatment. The results in Table A.4.2 of Appendix IV suggest that the three treatments (runsis 14.6, 147 and 14.8) have different means and therefore fall into different categoriesses. The overall mean $\overline{\overline{D_L}}$ and standard deviations are also reported in Table 3. This demonstrates that there is a distinct increase in the mean liquid dispersion coefficientnt, D_L, with superficial gas velocity. However, it is clear that the error, or standard deviations, are relatively high, indicating a wide spread in the model parameter D_L. We ascribe this to the inability of the ADM to describe accurately the measured tracer response.

In general, the overall magnitudes of the liquid phase axial dispersion coefficients suggest a reasonable degreeee of liquid (slurry) mixing in the column under the existing process rates. The characteristic liquid mixing time based on the entire dispersion height L is in the range LL^2/D_L : 350 - 650 seconds. The effect of this extent of mixing on reactor performaance naturally depends on the characteristic reaction time and level of conversion.

The liquid dispersion coefficients obtained in this study were compared with correlations from the literaturere (Kato et al., 1972; Baird and Rice, 1975; Deckwer et al., 1974). The correlations arre listed in Table 4. These are the few correlations that apply for the column diamneters and superficial gas velocities of interest to us. The liquid dispersion coefficientnts predicted by these correlations are in the range D_L : 1300 (U_G 14 cm/s) to 20000 (U_G 36 cm/s) cm^2/s. All the above correlations were obtained at atmospheric pressssure. Therefore a direct comparison cannot be made with the present experimental reresults, which were performed at elevated pressures. Clearly the correlations based on atatmospheric pressure data underpredict the observed liquid axial dispersion coefficientsts at all gas velocities.

There is evidence that g gas holdup in a bubble column increases at higher pressure due to an increase in the nnumber of small bubbles. The increase in gas density with pressure affects bubble formmation sizes, and bubble coalescence and breakup rates, all of which lead to smalleler bubble sizes (Wilkinson, 1991). This, in effect, delays transition from bubbly flooow to churn - turbulent flow (Krishna et al., 1991). At

[1] $\sigma = \sqrt{\sum(y-\overline{y})^2/(n-1)}$

Table 3: Results of ANOVA - Average D_L and Standard Deviations

Run	Injection	$\overline{D_L}$ cm^2/s	$\overline{\sigma_L{}^2}$ cm^2/s	$\overline{\overline{D_L}}$ cm^2/s	$\overline{\overline{\sigma_L}}$ cm^2/s
14.6	N1 - CEEN	2782	85		
	N1 - WWAL	4924	1191	4355	1532
	N2 - CEEN	5300	1499		
14.7	N1 - CEEN	1945	109		
	N1 - WWAL	3008	479	2713	678
	N2 - CEEN	3351	718		
	N2 - WWAL	2550	328		
14.8	N1 - CEEN	4764	343		
	N1 - WWAL	5219	258		
	N2 - CEEN	5529	381	5143	516
	N2 - WWAL	5057	822		

sufficiently high gas velocitieses, as in the runs studied in this report, a bubble column operating under high pressuure (3-5 MPa) is already in the churn turbulent regime, and the presence of a bimoddal bubble size distribution with large and small bubbles is usually seen (Krishna, 19994). It has been reported by Krishna et al. (1991) that beyond transition, in the chuurn turbulent regime, the gas holdup due to small bubbles is independent of gas velocitity. It is the holdup of the large bubbles that increases with increase in gas velocity. ·. However, the effect of pressure, and thereby gas density, on the holdup of these large b bubbles in the churn turbulent regime is negligible. As a result, at high pressures and l high gas velocities, the overall gas holdup is higher than in a reactor operating at atnmospheric pressure and the same gas velocity due to the excess of small bubbles in the.e system caused by delayed transition, while the holdup of large bubbles is comparable t to the holdup of large bubbles for similar gas velocities at atmospheric pressure (Krishnna et al., 1994). There is, hence, an additional interaction between the gas and liquid ε at high pressure. The axial dispersion coefficient is due to liquid recirculation and tuurbulent (radial and axial) mixing. Therefore, the liquid dispersion coefficient is expeected to increase with pressure at such high gas velocities.

Table 4: Correlations f for Liquid Dispersion Coefficient in Bubble Columns

Investigator	Equation (in SI)	Range of Variables
Kato and Nishiwaki (gas-liquid-solid))	$D_L = \frac{U_G D_c}{\frac{13Fr^{0.5}}{1+8Fr^{0.425}}}$ $Fr = \frac{U_G^2}{gD_c}$	$0.066 \leq D_c \leq 0.214$ m $0.02 \leq U_G \leq 0.3$ m/s
Baird and Rice (gas - liquid)l)	$D_L = 0.35\ D_C^{4/3}(gU_G)^{1/3}$	$0.003 \leq U_G \leq 0.45$ m/s $0.082 \leq D_C \leq 1.53$ m
Deckwer et al. (gas - liquid)	$D_L = 0.678 D_C^{1.4} U_G^{0.3}$	–

The relatively low increæase in D_L from U_G of 25 cm/s (Run 14.6 at 5.3MPa) to U_G of 36 cm/s (Run 14.8 at 3.6.6 MPa) may be accounted for by the decrease in pressure between the two runs, whickh to some extent masks the effect of U_G on the D_L obtained by fitting the tracer curve. .

5.1.2 Conclusions and l Future Work

The ADM, which has preesently been fitted only to the tracer data that do not exhibit overshoots, appears to provide satisfactory fits. However, there is a large variation in the axial dispersion coefefficient obtained at different detector levels, which is seen in standard deviations repported in Table 3. Our analysis clearly established the asymmetry of the actual reesponse, contrary to the ADM predictions, and the effect of injection point on the calcuulated liquid axial dispersion coefficient. All this indicates that while ADM may matdch a particular response well, it does not represent liquid mixing well.

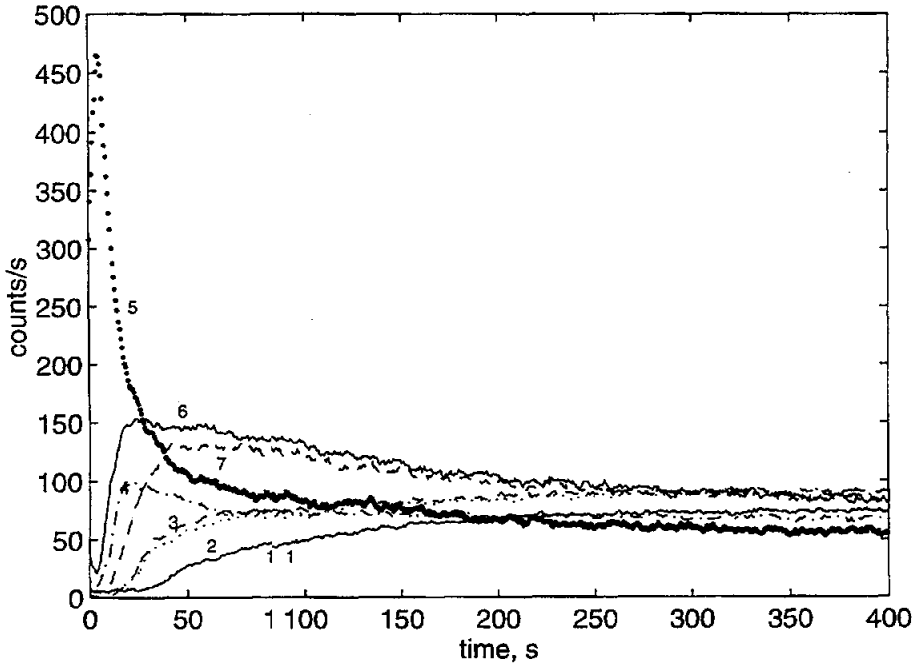

Figure 5: (a) Experimental DDetector Responses for Wall Injection at N 1 (Run 14.7)

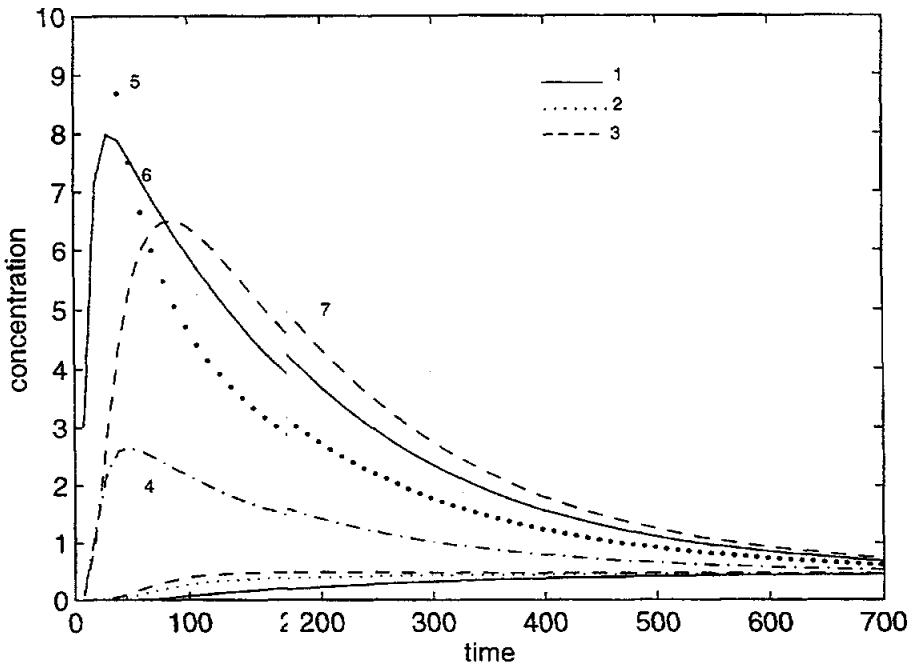

Figure 5: (b) Model Calculated Responses at Detector Levels (similar to experiment), for Qualitative Comparison with Fig 5(a) (time scale is arbitrary)

To match the data bettter, a phenomenological model that captures the essence of the fluid dynamic behavivior of the system should be used. The Recycle with Cross Flow and Dispersion Modelel (RCFDM) recently suggested by us (Degaleesan et al., 1996) provides an attractivive alternative in the description of liquid mixing. Preliminary analysis indicates thhat such a model, with a consistent set of parameters, is able to capture qualitativeely all the features of the experimentally observed tracer responses at various detectctor levels. Figure 5 exhibits the actual tracer responses and simulations based on the RRCFDM. The similarities between model and experiments are evident, as well as the a ability of the RCFDM for predicting a variety of responses at different column locatioons. Quantitative evaluation of parameters based on the RCFDM is part of the futuure planned work.

5.2 Gas Tracer

Two experiments were ccarried out at each process rate, with the gas tracer being injected at the inlet of the r reactor. The axial dispersion model is used to fit the data measured at all detector lelevels. Six types of parameter estimations were conducted with different sets of floatiiing parameters. For all cases, the liquid phase dispersion coefficient was fixed to the e value obtained from the liquid tracer experiments. The value of D_L used for eachh process rate was that obtained for the bottom center injection (N2 - center) withth the response measurement made at detector level 7. It was found that moderate clchanges in D_L do not affect the results of the model fits to data and the model paramneters for the gas tracer experiments significantly.

The ADM that describoes the spatial and temporal history of an injected soluble tracer is given by Equatioons 13, 14 and 15. The two coupled partial differential equations have to be solveed for the gas concentration, C_G, and liquid concentration, C_L. The temporal history ε at a given position z, of the combined response presented by Equation 7 has to be mnatched to the average detector response at the same axial location.

Parameter estimation isis again accomplished by minimizing the sum of the square of errors

$$\min_{P} \sum_{i=1}^{N_p} \left(\frac{R(t_i,z)}{R_{max}} - \frac{C_t(t_i,z)}{C_{tmax}}\right)^2 \tag{20}$$

where $R(t_i,z)$ is the averagge detector response at location z at time t_i, R_{max} is the maximum detector responsse at z. $C_t(t_i,z)$ is the total argon concentration defined by

Equation 7, evaluated at thee axial position z and time t_i, and $C_{t_{max}}$ is its maximum value at z. $\underline{P}$ is the vector obf parameters that is used to minimize the sum of square errors, and N_p is the numberr of data (sample) points, which is approximately 1000.

The model contains seveen parameters, D_L, D_G, ϵ_G, ϵ_L, H, K_La and U_G. Due to our consideration of the s slurry as pseudohomogeneous, $\epsilon_L = 1 - \epsilon_G$ so that the number of free parameters is s reduced to six. As already mentioned we take the liquid dispersion coefficient to be g given by the liquid phase tracer experiments. The five parameters D_G, ϵ_G, H, K_LLa and U_G have to be determined either by fitting the tracer data, or, from indepenndent observations or calculations. Thermodynamics can provide us with an estimatete for the Henry's constant, H. Holdup measurements can be used for estimation (of the average holdup, ϵ_G. Superficial gas velocity at the entrance and exit is knoown. With the exception of the gas superficial velocity, which is known to drop by 1 18% from the inlet value, and the Henry's constant H, which can be calculated reasonably accurately, none of the other parameters can be assessed ' a priori ' with certrtainty. We examined the ability of the model to match the observed tracer responsees based on several approaches using a different number of floating parameters as shoown in Table 5.

The following is a compavarison of the results obtained by each of the approaches represented as Case 1 - Case 6 6 in Table 5 and provides the rationale for each approach.

5.2.1 Case 1: Model witith Three Floating Parameters, D_G, H and K_La

In this case, ϵ_G (from DP f measurements) is used as input to the model, by considering the axial average holduup up to the measurement level ($\overline{\epsilon_{G,z}} = \int_0^L \epsilon_G dz/L$). This average at each level, z, is foound to vary only slightly from the overall average holdup reported in Table 1. Results s for the model parameters obtained by fitting the model to the various experimental r runs and detector levels are provided in Table 6. Figure 6 shows the results of fittingg the model responses to the experimental measurements at all the detector levels for r run 14.8-1. As in the case of liquid measurements, the fits of the model to the exprperimental data are in general very good. The fits for the remaining experiments aare shown in Appendix VI. In all the figures, there is an offset in the time axis, whichch is due to the differences in the zero time of recording the measurement (detectors)s) and the starting time of the tracer experiment. This is properly accounted for in thee model.

Table 5: Different Attemppts of Matching Model Predictions and Data at Various Detector Levels

Case No.	Fixed PParameters	Floating Parameters	Interpretation of Detector Response
1	$UU_G = U_{G,in}$ D_L = D_L(liquid) ϵ_G = $\overline{\epsilon_{G,z}}$ (DP)	D_G, K_La, H	Eqn 7
2a	$UU_G = U_{G,in}$ D_L = D_L(liquid) ϵ_G = $\overline{\epsilon_{G,z}}$ (DP) H == H(thermo)	D_G, K_La	Eqn 7
2b	$UU_G = U_{G,in}$ D_L = D_L(liquid) ϵ_G == $\overline{\epsilon_{G,z}}$ (NDG) H == H(thermo)	D_G, K_La	Eqn 7
3	$UU_G = U_{G,in}$ D_L = D_L(liquid) H == H(thermo)	D_G, K_La, ϵ_G	Eqn 7
4	$UU_G = U_{G,in}$ D_L = D_L(liquid) ϵ_G = $\overline{\epsilon_{G,z}}$ (DP)	D_G, K_La, α	$\alpha\epsilon_G C_G + \epsilon_L C_L$
5	$UU_G = U_{G,z}$ D_L = D_L(liquid) ϵ_G = $\overline{\epsilon_{G,z}}$ (DP) H == H(thermo)	D_G, K_La	Eqn 7
6	D_L = D_L(liquid) ϵ_G = $\overline{\epsilon_{G,z}}$ (DP) H == H(thermo)	D_G, K_La, U_G	Eqn 7

Table 6: Case 1: Parameters for Gas Phase Tracer Experiments

Run No.	U_G cm/s	Gas Holdup	D_L cm^2/s	Det. Lev.	Model Parameters		
					D_G cm^2/s	H	K_La s^{-1}
14.6-1	25.3	0.39	4696	1	9800	10.0	0.10
		0.39		2	6839	4.41	2.95
		0.38		3	7864	5.82	1.80
		0.37		4	5412	4.47	0.58
		0.38		5	7131	5.33	1.12
		0.39		6	5729	3.87	0.66
		0.40		7	6204	3.32	1.19
14.6-2		0.39		1	9396	10.0	0.10
		0.39		2	4446	4.28	1.16
		0.38		3	6229	5.82	2.50
		0.37		4	3337	3.70	0.56
		0.38		5	5455	4.65	0.79
		0.39		6	4649	3.78	0.49
		0.40		7	4356	3.41	0.65
14.7-3	14.3	0.34	3052	1	6987	10.0	0.10
		0.33		2	4219	4.35	1.69
		0.32		3	4663	5.11	1.58
		0.32		4	3402	4.75	0.43
		0.32		5	2466	3.76	0.56
		0.33		6	1681	3.98	0.56
		0.33		7	1816	3.17	0.63
14.7-4		0.34		1	6274	10.0	0.10
		0.33		2	3048	5.30	0.32
		0.32		3	4313	6.89	3.45
		0.32		4	2379	4.42	0.31
		0.32		5	1903	3.81	0.41
		0.33		6	1861	3.31	0.46
		0.33		7	1865	3.14	0.47
14.8-5	36.0	0.38	5925	1	9800	10.0	0.30
		0.37		2	5229	3.82	2.73
		0.37		3	6567	4.70	1.66
		0.37		4	4253	3.41	0.51
		0.37		5	4771	3.42	0.65
		0.38		6	4059	3.19	0.61
		0.38		7	3546	3.11	0.59
14.8-6		0.38		1	9800	10.0	0.20
		0.37		2	8531	6.80	2.47
		0.37		3	6505	6.85	3.01
		0.37		4	5070	3.61	0.36
		0.37		5	3793	3.41	0.51
		0.38		6	3106	3.21	0.54
		0.38		7	3985	3.00	0.60

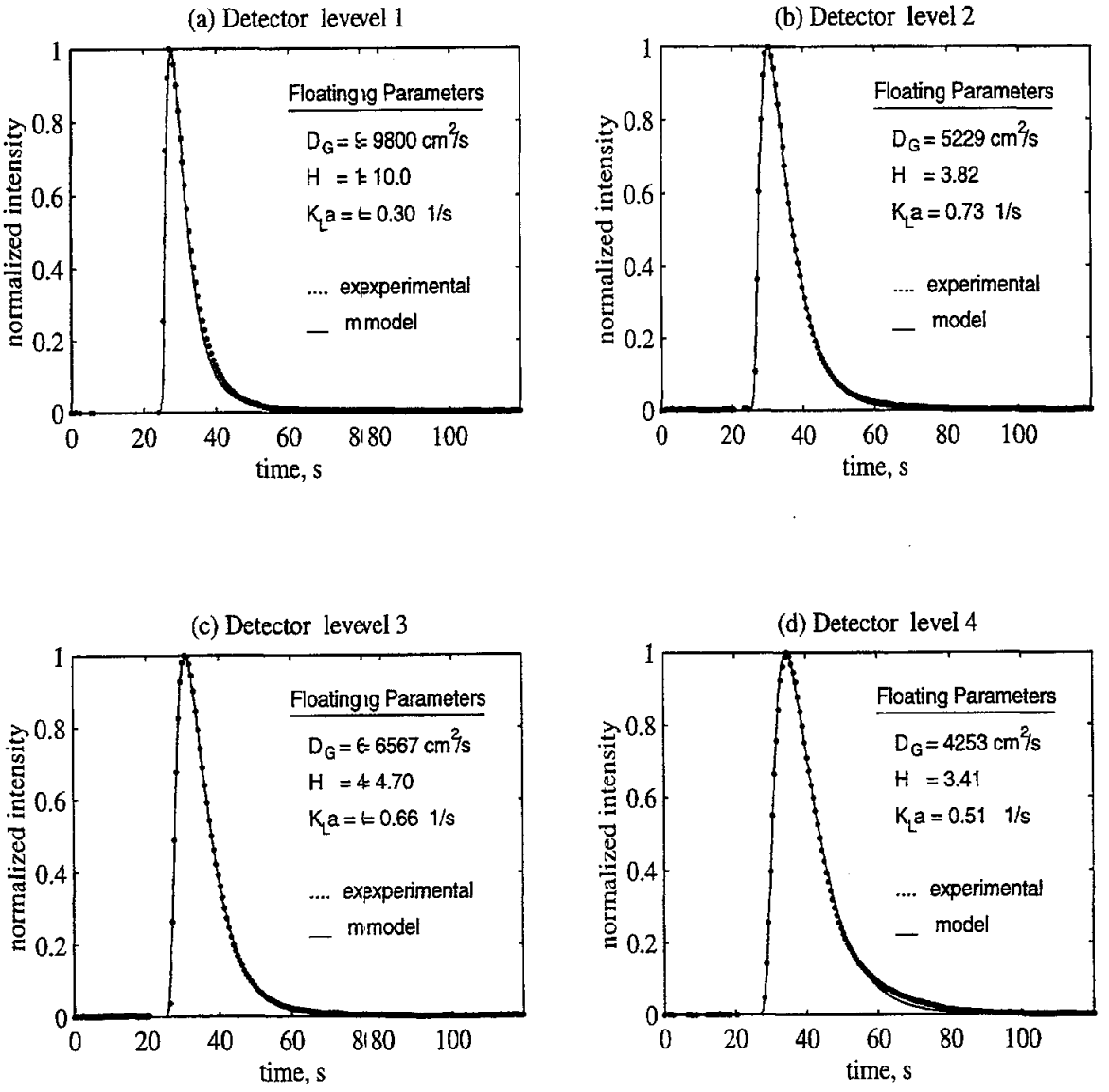

Figure 6: Gas Phase Impulilse Response for Case 1, Run 14.8-5, Injection Time 24.6s

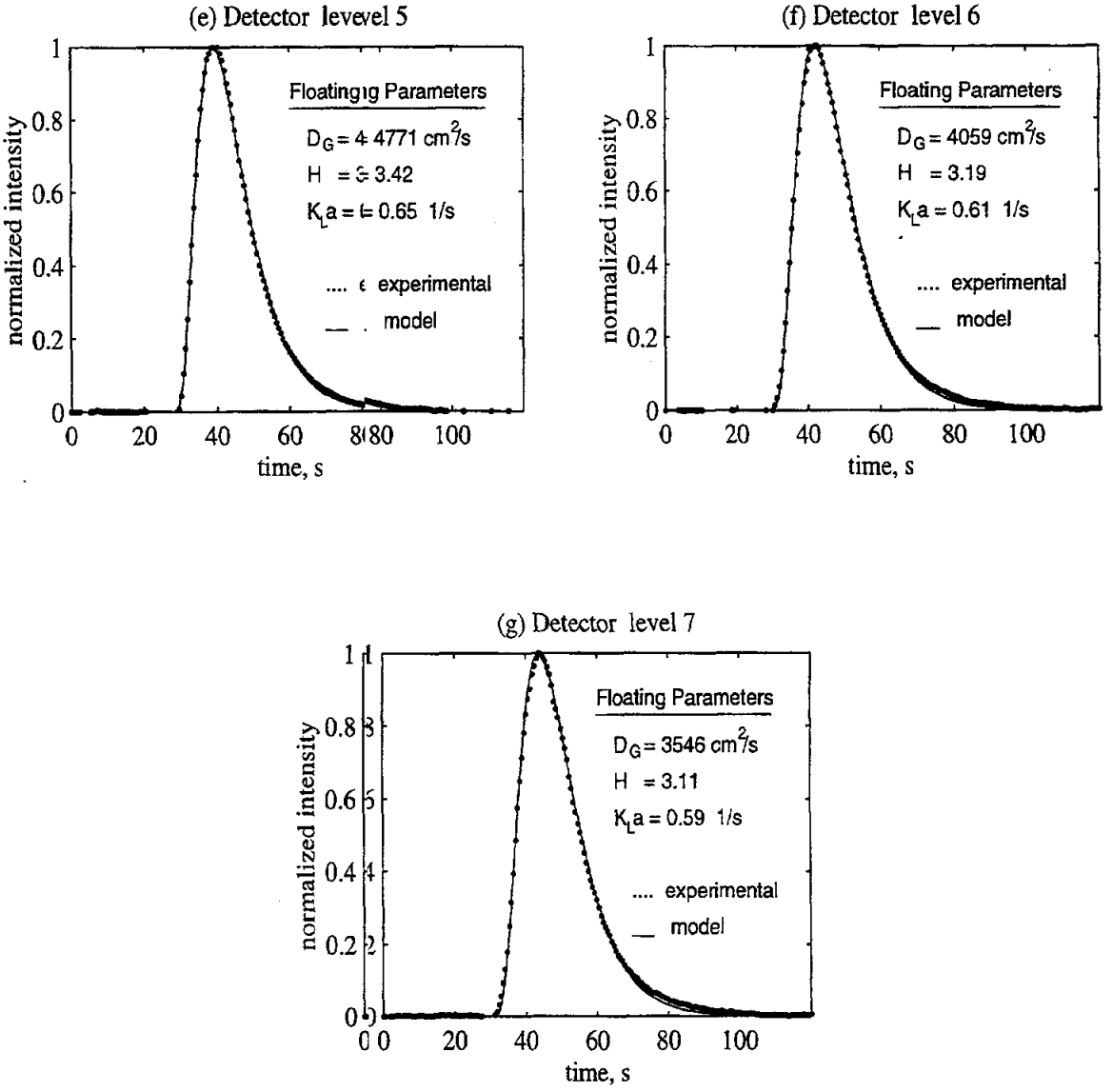

Figure 6 (contd.): Gas Phaase Impulse Response for Case 1, Run 14.8-5, Injection Time 24.6s

Discussion

For pipe flows, the ADDM is known to apply when the radial dispersion is significant enough to overcome the effects of convection. This criterion is expressed as $L/D_C \gg 0.08Pe_r$, where Pe_r is the radial dispersion Peclet number based on the radius of the tube. When applied to gas flow in bubble columns, $Pe_r = U_G R_c/\epsilon_G D_{rr}$, where D_{rr} is the radial turbulent diffusivity for the gas phase. This requires an independent evaluation of D_{rr}. Experimental measurements of D'_{rr}, the radial turbulent eddy diffusivity for the liquid are available using the CARPT (Computer Automated Radioactive Particle Tracking) technique in our laboratory, in smaller size columns (Degaleesan and Duduković, 1995). When extrapolated to larger diameter columns and higher superficial gas velocities (as in the present study), this yields estimated values of D_{rr} ($D_{rr} = D'_{rr}$).) in the range 100 - 150 cm^2/s based on the assumption that liquid and gas radial diffusivities are equal. This yields estimates of Pe_r in the range of 10 to 15, and indicates that the above criterion is well established for all higher detector levels. Even for the lowest detector (DET 1 in Figure 1), $L/D_c = 3.3$ is larger than 0.08 Pe_r, but not sufficiently large to fully justify the use of the ADM.

Using the gas phase axial dispersion coefficients obtained from parameter estimation calculations reported in Table 6, the dispersion Peclet numbers were calculated. For detectors at the farthestst level, $Pe \sim 25$, while for the the lowermost detector level, $Pe \sim 1$. Such a range of Peclet numbers suggests that the ADM is more suited at the highest detector levels, , where the flow can be considered to have small deviations from plug flow. It is the least suited at the lowermost levels. This may explain why the values of the parameters are quite consistent for the upper three to four levels of detectors, while for the lower levels, although the fits are good, there is a definite variation in parameter values. The parameters at the lowermost level ($L/D = 3.3$) were found to be very different from the other values.

A parametric sensitivity analysis was performed to study the sensitivity of the model to the various floating parameters. This analysis is performed by fixing two parameters at their fitted values and varying the third. The parameters were varied from -30% to +30% of their fitted values. Results for Run 14.8 - 1 at detector level 5 are shown in Figure 7. It is seen that the model is most sensitive to the Henry's constant H when compared with D_G and $K_L a$, and least sensitive to $K_L a$.

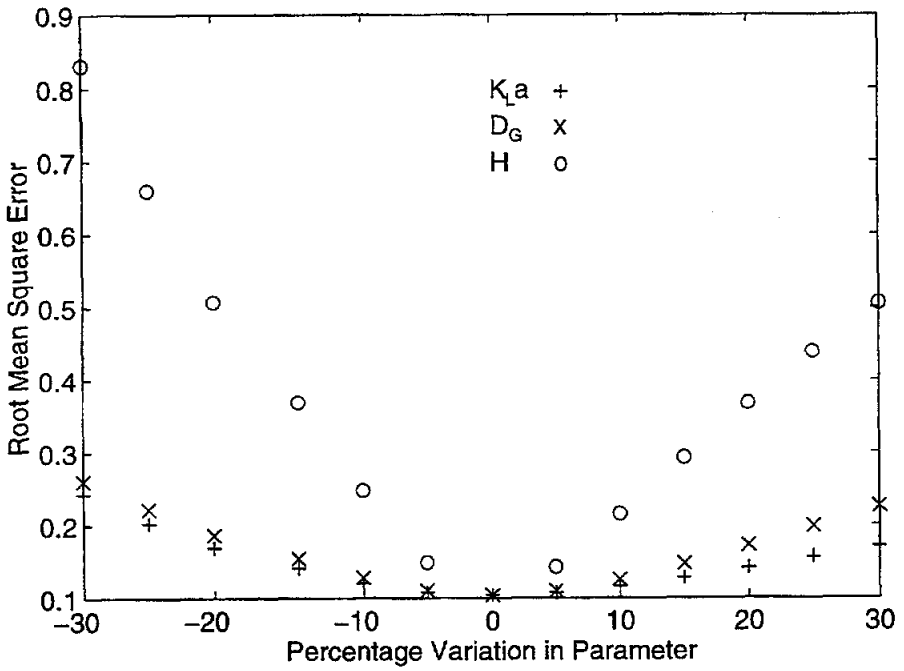

Figure 7: Results for Parametric Sensitivity Analysis for Run 14.8 - 5, Level 5

The mass transfer coefficicients and Henry's law constants obtained from the above described parameter estimatation (Table 6) are almost constant for all gas velocities at all the highest detector lelevels. Evaluation of the Henry's law constant from thermodynamic calculations yielelds values of 5.9 at 52 MPa, 250°C (run 14.6 and 14.7) and 8.1 at 36 MPa, 250°C ((run 14.8). The details of this calculation are shown in Appendix V. These values a are much higher than the model fitted values shown in Table 6. Thus, the results o obtained are suspect in spite of the excellent fits to the data. The constant "drift" o of H with detector position indicates problems in reconciling the model with the daata. Examination of Table 6 at each gas flowrate clearly indicates a trend in H and KK_La with detector position. For most of the runs there is also a trend in D_G.

Repeated runs at identicical conditions yielded variation in parameters. As with the liquid experiments, the ; results for all the three parameters are analyzed using ANOVA. It was found that t there is good repeatability for K_La and H for all the three runs (Table A.4.3). Fo'or D_G the repeatability for Runs 14.7 and 14.8 are good, but Run 14.6 is not satisfactctory. The analysis shows that the mean D_G from Runs 14.6-1 and 14.6 -2 belongs to o two different groups. This can be observed from Table 6, in which the dispersion coefefficients for Run 14.6-1 are generally higher than those for 14.6-2. In order to analalyze the effect of superficial gas velocity on each of the

parameters, the data from the two runs at each process rate is considered to belong to a group (same as for the liquid runs), and an ANOVA was performed for each parameter. The results in Table A.4.3 indicate that D_G varies with U_G. However, no dependence of K_La and HI on superficial gas velocity is seen.

5.2.2 Case 2: Model with Two Floating Parameters: D_G, K_La

Since the value of the Henry's constant, H, can be reliably obtained from thermodynamics, by fixing ϵ_G (from DP measurements) and H as model inputs, the model was fitted to the experimental data to estimate the remaining two unknown parameters, D_G and K_La. The parameters obtained by the fitting procedure are reported in Table 7.

Figure 8 (Appendix VI contains the figures for all the remaining runs) shows the model fit to the experimental results for Run 14.6-1 at all the detector levels. Clearly the fit of the model to the experimental data is the poorest at the detector level farthest from the point of injection, that is, close to the liquid-free surface, and gradually improves as one approaches the lower levels. Similar trends are seen for the other experimental runs as well. This behavior is counter intuitive, since it is expected that the farther the point of measurement is from the point of injection, the more applicable the axial dispersion model is.

If the gas holdup values for the upper levels are increased as input model parameters, the fits are considerably improved. A possible explanation for this behavior was sought as follows. When ϵ_G is taken to be erroneously low (ϵ'_G) for the case of the dispersion model, this implies that the front moves at a faster velocity (U_G/ϵ'_G) than it should. Using the three-parameter model of Case 1, there is more freedom for the model to predict a response similar to the experimental measurements. As shown earlier, the model is particularly sensitive to H. In Case 1, when the model predicts the pulse moving at a faster value of U_G/ϵ'_G than it should, H is made lower such that more tracer is in the liquid phase, which is in batch mode and has a high degree of mixing. Thus, the model is then capable of matching a broader spread in the tracer distribution with a larger mean residence time, as indicated by the experiment. However, when H is fixed (as is the situation in the present Case 2), the model loses this degree of freedom, and therefore the fits are not good.

Table 7: Case 2a: Parameters with Fixed H for Gas Phase Tracer Experiments

Run No.	U_G cm/s	Gas Holdup	D_L cm^2/s	Det. Lev.	H	Parameters	
						D_G cm^2/s	K_La s^{-1}
14.6-1	25.5.3	0.39	4696	1	5.86	9900	0.006
		0.39		2		7641	2.87
		0.38		3		7888	1.88
		0.37		4		7312	2.58
		0.38		5		7720	1.64
		0.39		6		6850	1.23
		0.40		7		5678	0.99
14.6-2		0.39		1	5.86	9006	0.006
		0.39		2		6040	7.32
		0.38		3		6285	2.75
		0.37		4		5750	7.32
		0.38		5		6772	2.28
		0.39		6		6421	1.52
		0.40		7		4868	1.11
14.7-3	14.4.3	0.34	3052	1	5.86	3345	3.22
		0.33		2		3228	0.70
		0.32		3		5540	0.94
		0.32		4		3114	0.65
		0.32		5		3241	1.17
		0.33		6		2977	1.41
		0.33		7		2987	1.58
14.7-4		0.33		1	5.86	2400	3.52
		0.33		2		2473	3.40
		0.32		3		2419	2.99
		0.32		4		2385	3.45
		0.32		5		2459	1.93
		0.33		6		2552	0.65
		0.33		7		2437	1.11
14.8-5	36.6.0	0.38	5925	1	8.11	16828	0.032
		0.37		2		11700	8.92
		0.37		3		11848	13.87
		0.37		4		10640	4.29
		0.37		5		10700	2.64
		0.38		6		7889	1.62
		0.38		7		6859	1.95
14.8-6		0.38		1	8.11	19832	0.0032
		0.37		2		10146	0.60
		0.37		3		10373	0.50
		0.37		4		11754	7.78
		0.37		5		9960	3.32
		0.38		6		8522	2.92
		0.38		7		7167	1.70

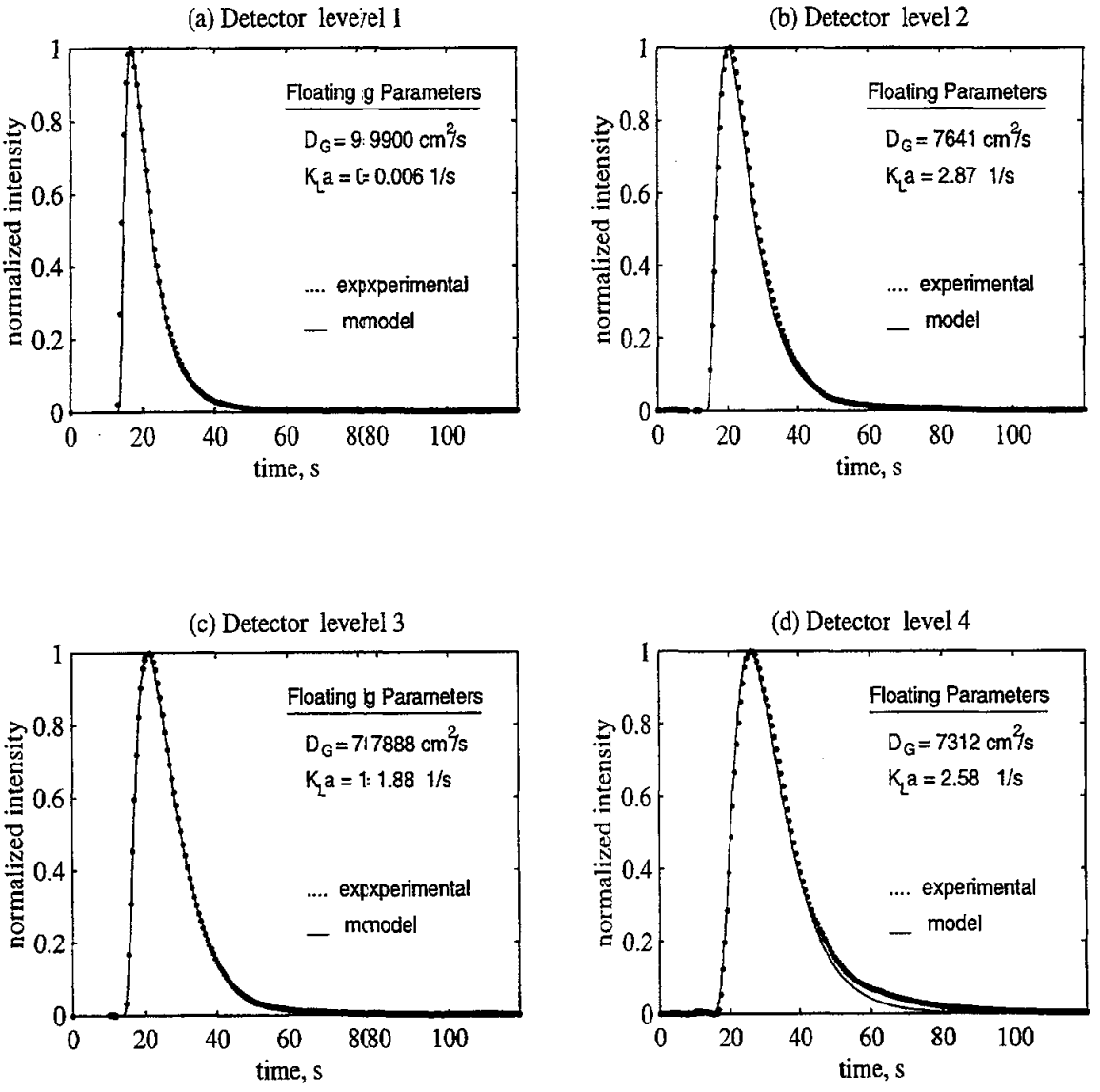

Figure 8: Gas Phase Impulilse Response for Case 2, Run 14.6-1, Injection Time 12.6s

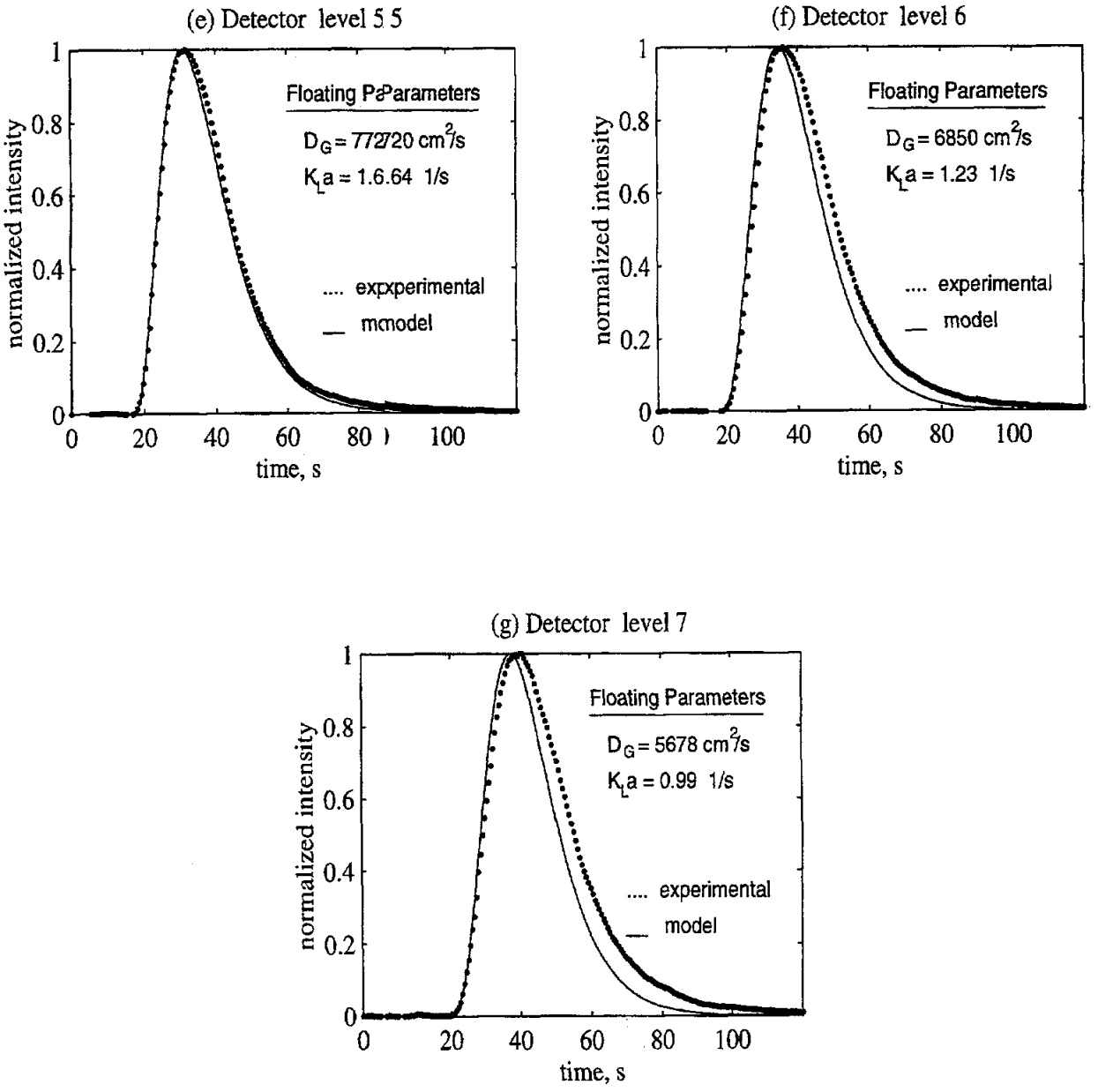

Figure 8 (contd.): Gas Phaase Impulse Response for Case 2, Run 14.6-1, Injection Time 12.6s

The increased holdup fofor which good fits are obtained, even in Case 2, are slightly higher than those reported d by DP, but are similar to the NDG measurements. Based on the DP measurements,s, the gas holdup starts increasing from detector level 4, which is expected to be ddue to foaming. When the system is foaming, the radial holdup distribution tends tto become more uniform, in which case the average holdup obtained from the NDG mmeasurements becomes more reliable. When the following radial gas holdup profile is s used (Kumar et al., 1994)

$$\epsilon_G(\xi) = \tilde{\epsilon_G}\frac{m+2}{m}(1 - c\xi^m) \tag{21}$$

with the exponent $m \geq 10.0$, the average holdup from NDG measurements becomes quite accurate. This is illusstrated in Figure A.1.2 in Appendix I, in which a comparison is shown of the NDG-b-based average and a true cross-sectional average.

In order to accept the l NDG measurements as a better indication of the average holdup, one would have to s show that the DP measurements are inaccurate in a foaming system with solids (sinnce there is such a large discrepancy between the holdups from the two measurementits). We do not have such evidence at present. However, it is clear that better fits cann be obtained for the data with fixed H values using the measurements from NDG fcfor the average holdup estimates at the higher detector levels. The parameters estimaated under such conditions are provided in Table 8. Figure 9 shows the results for Runn 14.6-1 (compare with Figure 8 (e) - (f)). Hence, based on the premise that NDG-basesed holdup measurements in the foaming region are more accurate than their DP coounterpart, reasonable fits are obtained. However, there is no independent experimentntal verification for the existence of the flat radial holdup profiles in the upper part c of the reactor. Therefore, the above approach cannot be completely justified at presssent.

The above analysis showws that the model is very sensitive to H as well as ϵ_G. It is unable to match the tracer c data well when only two unknown parameters are assigned if one or both of the chosemn parameters may be in error.